

Design-oriented strength and strain models for GFRP-wrapped concrete

Housseem Messaoud*, Amar Kassoul^a and Abdelkader Bougara^b

Laboratory of Structures, Geotechnics and Risks (LSGR), Department of Civil Engineering, Hassiba Benbouali University of Chlef, Algeria

(Received March 27, 2020, Revised August 12, 2020, Accepted September 11, 2020)

Abstract. The aim of this paper is to develop design-oriented models for the prediction of the ultimate strength and ultimate axial strain for concrete confined with glass fiber-reinforced polymer (GFRP) wraps. Twenty of most used and recent design-oriented models developed to predict the strength and strain of GFRP-confined concrete in circular sections are selected and evaluated basing on a database of 163 test results of concrete cylinders confined with GFRP wraps subjected to uniaxial compression. The evaluation of these models is performed using three statistical indices namely the coefficient of the determination (R^2), the root mean square error (RMSE), and the average absolute error (AAE). Based on this study, new strength and strain models for GFRP-wrapped concrete are developed using regression analysis. The obtained results show that the proposed models exhibit better performance and provide accurate predictions over the existing models.

Keywords: glass fiber-reinforced polymer (GFRP); confined concrete; strength model; strain model; statistical analysis

1. Introduction

Among the techniques employed for strengthening and retrofitting of concrete structures, fiber-reinforced polymer (FRP) is currently widely used and accepted in the civil engineering community (e.g., Ding *et al.* 2018, Hou *et al.* 2015, Sumathi and Vignesh 2017). From its beneficial properties such as high strength-to-weight ratio, high resistance to aggressive environmental conditions, ease and speed of application, providing great improvement in both strength and ductility to concrete columns is the most important advantage (Bakis *et al.* 2002, Wu *et al.* 2012).

Numerous experimental studies have been carried out to understand the compressive behavior of concrete confined with FRP. At the beginning, the steel and active confinement models of Mander *et al.* (1988), Newman and Newman (1972), and Richart *et al.* (1928) were suggested to model FRP-confined concrete by Fardis and Khalili (1981, 1982), and Saadatmanesh *et al.* (1994). However, this approach has been shown to be disadvantageous where many studies have recognized the differences in the stress-strain behavior of FRP-confined and steel-confined concrete (Mirmiran *et al.* 1996, Miyauchi *et al.* 1997, Saafi *et al.* 1999, Samaan *et al.* 1998, Spoelstra and Monti 1999). Consequently, a large number of experimental studies were carried out to model the behavior of concrete confined with various type of FRP, leading to a large experimental data (e.g., Hou *et al.* 2015, Jiang and Teng 2007, Lam and Teng

2004, Shehata *et al.* 2002, Vincent and Ozbakkaloglu 2013) for Carbon-FRP (CFRP), (Almusallam 2007, Cui and Sheikh 2010, Elwan and Omar 2014, Youssef *et al.* 2007) for Glass-FRP (GFRP), (Dai *et al.* 2011, Ozbakkaloglu and Akin 2012, Wang and Wu 2011, Wu and Wang 2010) for Aramid-FRP (AFRP)). Basing on that, many strength and strain models were suggested by researchers. Diverse-use models that are devoted for common types of FRP confinement were largely proposed (e.g., Al Abadi *et al.* 2016, Cascardi *et al.* 2017, Fahmy and Wu 2010, Ilki *et al.* 2004, Lam and Teng 2003, Lim *et al.* 2016, Realfonzo and Napoli 2011). Also, models that are specific for certain FRP type and confinement technique such as Benzaid *et al.* (2010), Mesbah and Benzaid 2017, Rashid and Aboutaha (2014), Wu *et al.* (2006), Xiao and Wu (2000) for CFRP-confined concrete; Arabshahi *et al.* (2020), Djafar-Henni and Kassoul (2018), Wu and Wang 2010, and Wu *et al.* 2009, for AFRP-confined concrete were also proposed since the FRP have different behaviors according to the type of the fiber as can be seen in Fig. 1. However, few models were dedicated to GFRP confinement such as those of Huang *et al.* (2016) and Touhari and Mitiche-Kettab (2016) that were developed for GFRP wraps and tubes.

CFRP has the highest tensile strength and modulus of elasticity among the other types, however it has the highest price as they tend to be 10 to 30 times more expensive than GFRP (Sonnenschein *et al.* 2016). Although GFRP provide lower strength and ductility compared to CFRP and AFRP, it is the most used in industry due to its low price. Despite that, no researchers have predicted strength and strain models of confined concrete columns with GFRP-wraps only except Touhari and Mitiche-Kettab (2016).

This paper treats 20 of the most used and recent existing design-oriented models that were developed to predict the ultimate strength and strain of GFRP-confined concrete. The models were evaluated using a database of 163 compression test results of GFRP-wrapped normal and

*Corresponding author, Ph.D. Student

E-mail: h.messaoud@univ-chlef.dz

^aProfessor

E-mail: am.kassoul@univ-chlef.dz

^bProfessor

E-mail: a.bougara@univ-chlef.dz

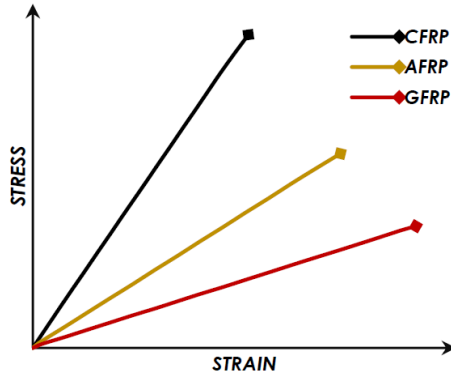


Fig. 1 Typical stress-strain curves of some FRP composite materials

high-strength concrete cylinders assembled from the literature. Using regression analysis, new design-oriented strength and strain models for concrete columns confined with GFRP-wraps only are proposed. Finally, to show the validity of the proposed models, comparisons with experimental data and with the considered models are performed.

2. Experimental test database

A database of experimental tests performed on short concrete columns confined with glass-fiber reinforced polymer wraps is collected through an extensive review of the literature. The test results were chosen basing on the set of selection criteria listed below, which resulted to the selection of 163 test data from 27 experimental studies as shown in Table 1 (Appendix 1). The selection criteria aimed to ensure the reliability and the consistency of the analysis:

- Specimens with unconfined concrete strength ranging from normal to high strength (9.3 to 128 MPa) were considered.
- Specimens with a height-to-diameter ratio greater than three were excluded, to eliminate the influence of specimen slenderness.
- Specimens with no and/or negligible strength and/or strain improvement were excluded.
- Specimens with either transverse and/or longitudinal steel or internal GFRP reinforcement were excluded.
- Only specimens confined with GFRP sheets were included (i.e., concrete-filled GFRP tubes were excluded).
- Only specimens confined with continuous GFRP were included (i.e., partially GFRP-wrapped specimens were excluded)
- Only specimens wrapped with GFRP wraps having fibers oriented in the hoop direction were included.
- Only specimens failed due to the rupture of the GFRP wrap were included.

The database includes for each specimen: the dimensions of the specimen (height h (mm), diameter d (mm), and the ratio h/d); the properties of concrete (strength of unconfined concrete f'_{co} (MPa) and its corresponding strain ε_{co} (%)); The properties of GFRP (elastic modulus E_f (GPa), maximum tensile strength

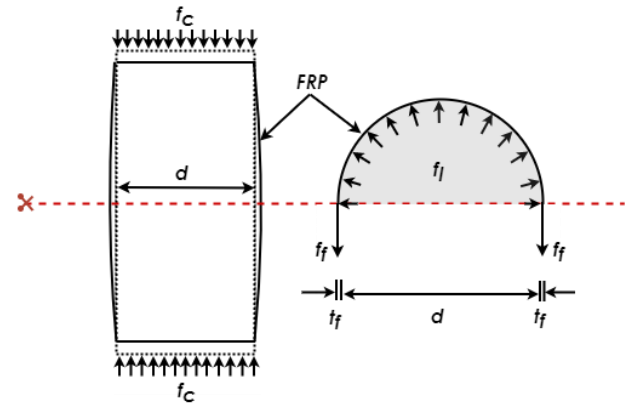


Fig. 2 Confinement mechanism in FRP-confined concrete

f_f (MPa), total thickness t_f (mm), the ultimate tensile strain ε_f (%)); The ultimate measurements of confined concrete (axial strength f'_{cc} (MPa) and axial deformation ε_{cc} (%), the rupture deformation of the GFRP $\varepsilon_{h,rupt}$ (%), the strain efficiency factor k_ε , and the confinement effectiveness strength and strain ratios (f'_{cc}/f'_{co}) and ($\varepsilon_{cc}/\varepsilon_{co}$) respectively).

3. Compressive behavior of FRP-confined concrete

When concrete cylinders confined with FRP wraps are subjected to axial compression, the concrete follows a behavior similar to that of unconfined concrete at low strain levels. However, with the increase of the axial load, the concrete starts to dilate and push against the FRP (Lam and Teng 2003). The FRP generates a passive confining pressure to restrain the gradual dilation of the concrete. This stress condition puts the concrete in a triaxial state of stress until failure of the FRP as shown in Fig. 2.

Based on the confinement mechanism drawn in Fig. 2, the maximum confinement stress (f_l) generated by the FRP is expressed as shown in Eq. (1)

$$f_l = \frac{2t_f f_f}{d} = \frac{\rho_f f_f}{d} = E_l \varepsilon_f \quad (1)$$

Where (ρ_f) and (E_l) are the volumetric ratio and the lateral stiffness of the FRP expressed in Eqs. (2)-(3) respectively

$$\rho_f = \frac{4t_f}{d} \quad (2)$$

$$E_l = \frac{2E_f t_f}{d} \quad (3)$$

It has been observed that the FRP ruptures at a strain ($\varepsilon_{h,rupt}$) lower than its ultimate strain (ε_f) (De Lorenzis and Tefers 2003, Lam and Teng 2003, Pessiki *et al.* 2001, Shahawy *et al.* 2000, Spoelstra and Monti 1999, Xiao and Wu 2000). A strain factor (k_ε) was proposed to account for this reduction (Lam and Teng 2003, Pessiki *et al.* 2001). Therefore, the confinement stress at rupture ($f_{l,rupt}$) is expressed as follows (Eq. (4))

$$f_{l,rup} = \frac{2t_f E_f \varepsilon_{h,rup}}{d} = \frac{2t_f E_f k_\varepsilon \varepsilon_f}{d} = \rho_K \rho_\varepsilon f'_{co} \quad (4)$$

Where (ρ_K) and (ρ_ε) are the stiffness and the strain ratios of the FRP relative to that of the concrete expressed as shown in Eqs. (5)-(6) respectively.

$$\rho_K = \frac{2t_f E_f}{d(f'_{co}/\varepsilon_{co})} \quad (5)$$

$$\rho_\varepsilon = \frac{\varepsilon_{h,rup}}{\varepsilon_{co}} \quad (6)$$

4. Existing strength and strain models

A review of the existing literature is carried out for the investigation of the available confinement models developed for circular GFRP-confined concrete. This resulted in the selection of 20 widely used and recent strength and strain models. Their expressions are given by the confinement effectiveness strength and strain ratios (f'_{cc}/f'_{co}) and $(\varepsilon_{cc}/\varepsilon_{co})$ respectively as shown in Table 2 (Appendix 2).

5. Evaluation of the existing models

5.1 Statistical analysis

The performance of the existing strength and strain models is evaluated by comparing their predictions with the experimental data reported in Table 1. Three statistical indices namely the coefficient of the determination (R^2), the root mean square error ($RMSE$), and the average absolute error (AAE) expressed in Eqs. (7)-(9) are used in the assessment.

$$R^2 = \left(\frac{\sum(x - \bar{x})(y - \bar{y})}{\sqrt{\sum(x - \bar{x})^2 \sum(y - \bar{y})^2}} \right)^2 \quad (7)$$

$$RMSE = \sqrt{\frac{\sum(x - y)^2}{n}} \quad (8)$$

$$AAE = \frac{\sum \left| \frac{x - y}{y} \right|}{n} \quad (9)$$

where (x) and (y) are the experimental and the predicted value, respectively; (\bar{x}) and (\bar{y}) are the average of the experimental and predicted values, respectively, and (n) is the total number of the datasets.

Ranging from 0 to 1, (R^2) is used to evaluate the relationship between predicted and experimental values, where high values indicate better fit. It should be noted that ($R^2 = 1$) does not guarantee a perfect prediction, it shows only that there is a linear correlation between predicted and experimental values (Sadeghian and Fam 2015).

($RMSE$) and (AAE) are used to indicate how close are the predicted values to the experimental values. Low values of ($RMSE$) and (AAE) indicate accurate prediction.

Each model was assessed against all the test results included in the database, unless specific limitations or specific equations for certain test parameters are specified by the model. These specifications include: method of confinement (i.e., wraps, wraps and tubes), type of FRP material (i.e., diverse FRP, GFRP, GFRP and CFRP), unconfined concrete strength (f'_{co}), strain efficiency factor (k_ε), and strain at unconfined concrete strength (ε_{co}). Each of these limitations are considered in the performance assessment of the models.

As shown in Table 2, specifications are reported for each model, where some models were only applicable to certain FRP type or confinement techniques (e.g., Huang *et al.* 2016, Saadatmanesh *et al.* 1994, Touhari and Mitiche-Kettab 2016, Xiao and Wu 2003), while others were applied to certain unconfined concrete strength ranges (f'_{co}) (i.e., Berthet *et al.* 2006, Fahmy and Wu 2010). There were also a group of models that specified certain coefficients and equations for certain parameters such as the strain efficiency factor (k_ε) (Baji *et al.* 2016, Matthys *et al.* 2006, Touhari and Mitiche-Kettab 2016, Xiao and Wu 2003), and the strain at unconfined concrete strength (ε_{co}) (Lim *et al.* 2016).

5.2 Strain efficiency factor

Since the values of the strain efficiency factor (k_ε) required by the majority of the reported models for the calculation of the rupture confinement stress ($f_{l,rup}$) and the strain ratio (ρ_ε) are often not provided in the available test results, prediction of the omitted values is performed in this study.

Analyzing the experimental results of (k_ε), it is observed that (k_ε) depends on the properties of the GFRP and the unconfined concrete strength. It was found that increase in (f_f) results in a decrease in the strain reduction factor, whereas an increase in (f'_{co}) results in an increase in (k_ε). Other studies such as that of Ozbakkaloglu and Akin (2012) for CFRP and AFRP-confined concrete, and that of Lim and Ozbakkaloglu (2014) for FRP-wrapped and tube-encased concrete showed that an increase in (f'_{co}) results in a decrease of (k_ε), which is the opposite of the observation reported above in this study. Using regression analysis, the influence of these two parameters resulted in the expression shown in Eq. (10) for the calculation of the strain reduction factor.

$$k_\varepsilon = 0.645 + 1.49 f'_{co} \times 10^{-3} + \frac{15.5}{f_f} - 15.13 f_f^2 \times 10^{-8} \quad (10)$$

where (f'_{co}) and (f_f) are in MPa.

The statistical evaluation demonstrates a strong correlation ($R^2 = 0.85$) with the experimental results and very low errors ($RMSE = 0.05$) and ($AAE = 0.04$) for this equation, which indicates an accurate fit between experimental and predicted values.

5.3 Performance assessment of the existing strength models

Table 3 Performance of selected strength and strain models

No.	Source	Strength model			Strain model		
		R^2	RMSE	AAE	R^2	RMSE	AAE
1	Saadatmanesh <i>et al.</i> (1994)	0.52	0.65	0.55	0.10	4.69	3.33
2	Karbhari and Gao (1997)	0.65	0.42	0.31	0.26	6.68	5.20
3	Toutanji (1999)	0.65	0.83	0.69	0.18	10.10	7.85
4	Moran and Pantelides (2002)	0.66	1.05	0.81	0.12	10.07	8.82
5	Xiao and Wu (2003)	0.69	0.99	0.65	0.23	5.00	3.42
6	Bisby <i>et al.</i> (2005)	0.69	0.40	0.28	0.26	6.24	4.78
7	Matthys <i>et al.</i> (2005)	0.55	0.50	0.38	0.07	6.53	4.89
8	Berthet <i>et al.</i> (2006)	0.63	0.53	0.35	0.31	4.07	3.12
9	Wu <i>et al.</i> (2006)	0.26	0.75	0.52	0.15	6.08	4.00
10	Ciupala <i>et al.</i> (2007)	0.64	0.81	0.69	0.65	3.13	2.30
11	Youssef <i>et al.</i> (2007)	0.67	0.49	0.37	0.23	5.12	3.57
12	Fahmy and Wu (2010)	0.72	0.47	0.34	0.09	5.12	3.65
13	Pham and Hadi (2014)	0.58	0.78	0.63	0.11	6.45	4.85
14	Sadeghian and Fam (2015)	0.47	0.47	0.37	0.13	4.71	3.38
15	Touhari and Mitiche-Kettab (2016)	0.66	0.48	0.36	0.23	4.49	3.26
16	Huang <i>et al.</i> (2016)	0.52	0.61	0.42	0.16	6.97	5.33
17	Baji <i>et al.</i> (2016)	0.57	0.49	0.35	0.13	5.68	3.91
18	Lim <i>et al.</i> (2016)	0.73	1.07	1.00	0.23	4.70	3.13
19	Keshtegar <i>et al.</i> (2017)	0.53	0.45	0.33	0.16	4.52	3.19
20	Fallah Pour <i>et al.</i> (2018)	0.67	0.44	0.30	0.23	4.59	3.03

The strength models shown in Table 2 are examined using the statistical parameters described above using 163 experimental data collected in Table 1. The obtained results are summarized in Table 3.

According to Table 3, the strength models show an average (R^2) of 0.60 in predicting the experimental data, which indicates a fair forecast. (R^2) ranges between 0.73 and 0.26 for the models of Lim *et al.* (2016) and Wu *et al.* (2006) respectively, which shows that the first model proves the best fit compared to the other 19 models. However, this model shows low accuracy, where the minimum values of errors ($RMSE = 0.40$) and ($AAE = 0.28$) which are the closest to 0 are recorded by the model of Bisby *et al.* (2005) proving its high accuracy over the other models. Fig. 3 illustrates the performance of these two strength models. Although the model of Lim *et al.* (2016) provides the best (R^2), its predictions are totally biased from the line of the perfect fit (45°) showing underestimation of the experimental results (see Fig. 3). On the other hand, the model of Bisby *et al.* (2005) shows a good dispersion of the data around the reference line (45°) but its ($R^2 = 0.69$) is less than the best value. From this analysis, it can be concluded that there is no model gives the best statistical indices showing good performance, even the model exclusively developed for GFRP-wrapped concrete of Touhari and Mitiche-Kettab (2016).

5.4 Performance assessment of the existing strain models

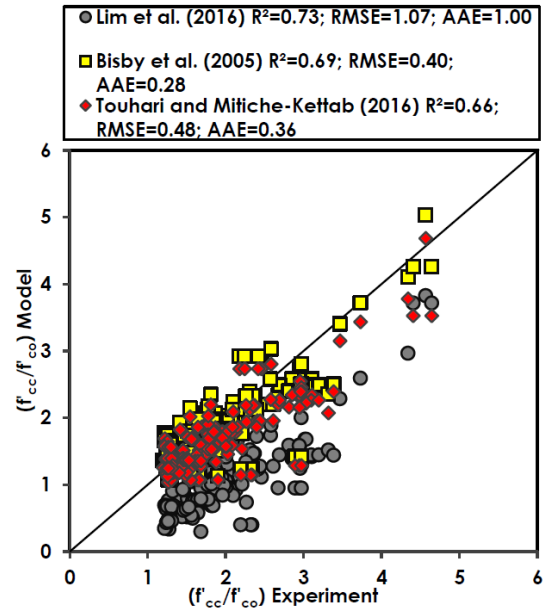


Fig. 3 Performance of three existing strength models

Statistical results of the performance analysis of the 20 strain models shown in Table 2 using the collected database are presented in Table 3. From this table, the coefficient of determination (R^2) for these models varies between 0.65 and 0.07, with an average of 0.20. This shows reduced fit comparing to their corresponding strength models. The model of Ciupala *et al.* (2007) shows the top ($R^2 = 0.65$) proving the best fit with the experimental data and provides the minimum values of the error indices ($RMSE = 3.13$) and ($AAE = 2.3$) which indicates that this model is the best accurate one compared to the other 19 strain models. Fig. 4 illustrates the performance of this model with the model of Touhari and Mitiche-Kettab (2016). The figure shows that although the model of Ciupala *et al.* (2007) is the best accurate model, it shows high values of errors and low accuracy in predicting the experimental results as illustrated by a large dispersion of the data around the reference line (45°). Based on this analysis, there is no model with an accuracy reflecting a good performance in predicting the ultimate strain, even the model of Touhari and Mitiche-Kettab (2016) that was based only on GFRP-wrapped concrete test results.

6. Proposed models for GFRP-wrapped concrete

After review of the selected strength and strain models and showing their performance in the prediction of the ultimate condition (f'_{cc} , ϵ_{cc}) of GFRP-wrapped circular concrete columns, improved design-oriented models are proposed in this section. The models were obtained through calibration of variable number of parameters (e.g. f'_{co} , $f_{l,rupt}$) which influences the level of accuracy obtained regarding the targeted parameters (i.e. (f'_{cc}/f'_{co}) and ($\epsilon_{cc}/\epsilon_{co}$)).

The calibration of the models is performed on the basis of a general regression analysis of the reported experimental

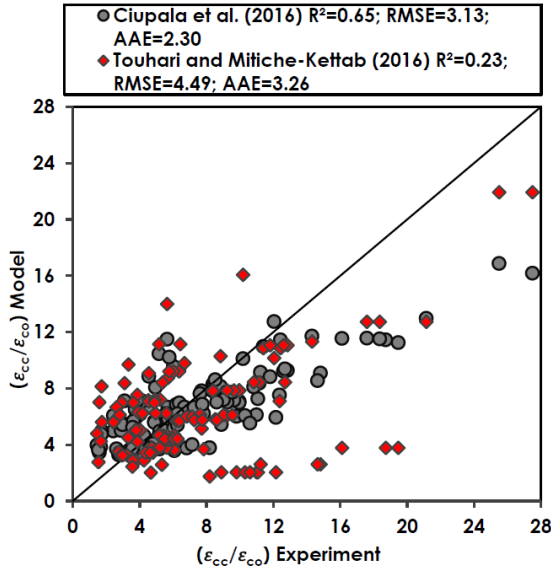


Fig. 4 Performance of two existing strain models

database. The regression analysis is based on minimization of errors. No limits on the form of the model and the number of parameters are imposed, and hence, an endless heavy iterative procedure is unavoidable. To that end, the regression analysis was performed using a data analysis engine (Eureqa software (Schmidt and Lipson 2009)).

6.1 Proposed strength model

Basing on the analysis of the experimental results reported in the collected database and referring to the equations and the performance of the assessed strength models, and after consideration of a wide range of parameters that were covered by the experimental database, the parameters observed to have high influence on the strength effectiveness of GFRP-wrapped concrete specimens are: the unconfined concrete strength (f'_{co}), the strain ratio (ρ_ϵ), and the stiffness ratio (ρ_K).

These parameters are inter-related as shown in Eq. (11)

$$\frac{f_{l,rup}}{f'_{co}} = \rho_K \rho_\epsilon \quad (11)$$

Through consideration of a large number of cases, the following empirical relationship was derived for the ultimate stress (Eq. (12))

$$\frac{f'_{cc}}{f'_{co}} = 0.775 + \frac{15.8}{f'_{co}} + \rho_K \left(4.34 \rho_\epsilon + \frac{24.5}{\rho_\epsilon} - 16.4 \right) \quad (12)$$

This relationship can be written as a function of the confinement ratio ($f_{l,rup}/f'_{co}$) as the majority of the existing models which were based on the general form of the expression proposed by Richart *et al.* (1928) (Eq. (13))

$$\frac{f'_{cc}}{f'_{co}} = c_1 + k_1 \frac{f_l}{f'_{co}} \quad (13)$$

Where, (c_1) is a calibration constant, and (k_1) is a strength enhancement coefficient. Several models have modified this equation and proposed nonlinear and power

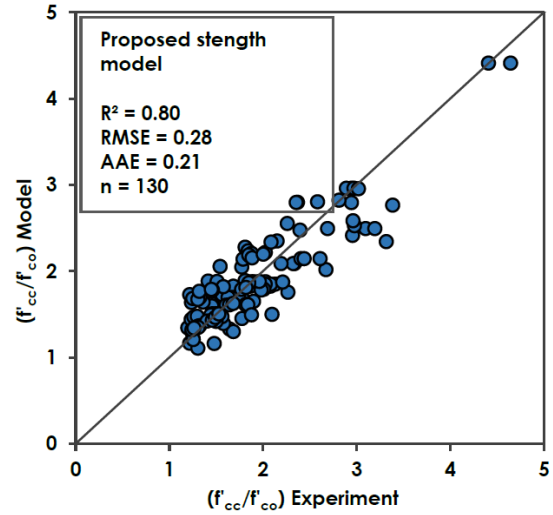


Fig. 5 Performance of the proposed strength model

equations of the confinement ratio (f_l/f'_{co}) (e.g., Saadatmanesh *et al.* 1994, Toutanji 1999, Wu *et al.* 2006, Xiao and Wu 2003).

The proposed strength model used the same form as these existing models, where (k_1) is expressed as a function of the strain ratio (ρ_ϵ), as shown in Eq. (14)

$$\frac{f'_{cc}}{f'_{co}} = 0.775 + \left(4.34 - \frac{16.4}{\rho_\epsilon} + \frac{24.5}{\rho_\epsilon^2} \right) \frac{f_{l,rup}}{f'_{co}} + \frac{15.8}{f'_{co}} \quad (14)$$

Where, an increase in (f'_{co}) shows an adverse influence on (f'_{cc}/f'_{co}) as reported by the exiting literature.

6.2 Validation of the proposed strength model

The accuracy of the proposed model is evaluated and compared with the 20 strength models assessed previously. The statistical indices defined in section (5.1) are used in the comparison. Fig. 5 illustrates the performance of the proposed strength model with respect to the collected database. It can be seen that predictions of the proposed strength model are in good agreement with the experimental data with a high correlation ($R^2 = 0.80$), and small indices of errors ($RMSE = 0.28$, and $AAE = 0.21$) that tend towards 0 indicating a good accuracy and well distributed data points around the (45°) line.

Comparison of the statistical indices (R^2 , $RMSE$, and AAE) of the proposed model and the 20 strength models is shown in Figs. 6(a)-(c) respectively. Fig. 6(a) illustrates that the proposed strength model provides the best fit of the experimental data compared to the other models where the model of Lim *et al.* (2016) is the best fitting of the existing models offered ($R^2 = 0.73$). In the same context, all the assessed models such as the best accurate model of Bisby *et al.* (2005) with ($RMSE = 0.40$, and $AAE = 0.28$) show considerably low accuracy comparing to the proposed model which offers substantially the lowest indices of errors as shown in Figs. 6(b)-(c) respectively. Therefore, it can be concluded that the proposed model is more effective in predicting the ultimate strength of GFRP-wrapped concrete.

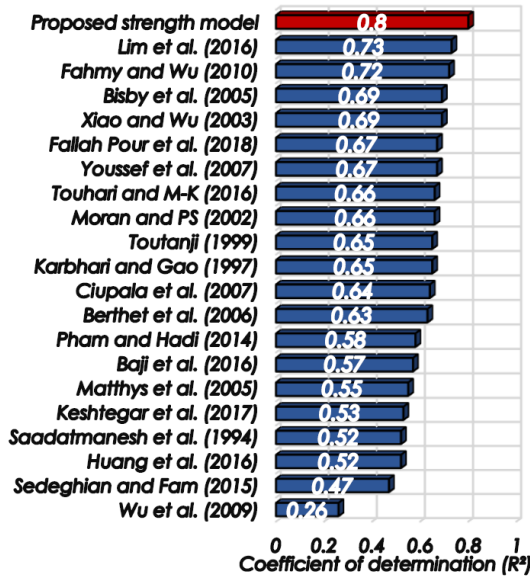


Fig. 6(a) Comparison of coefficient of determination (R²) of the proposed and existing strength models

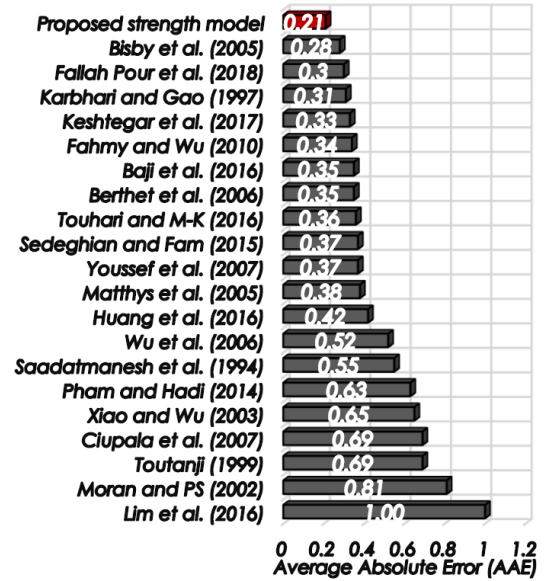


Fig. 6(c) Comparison of average absolute error (AAE) of the proposed and existing strength models

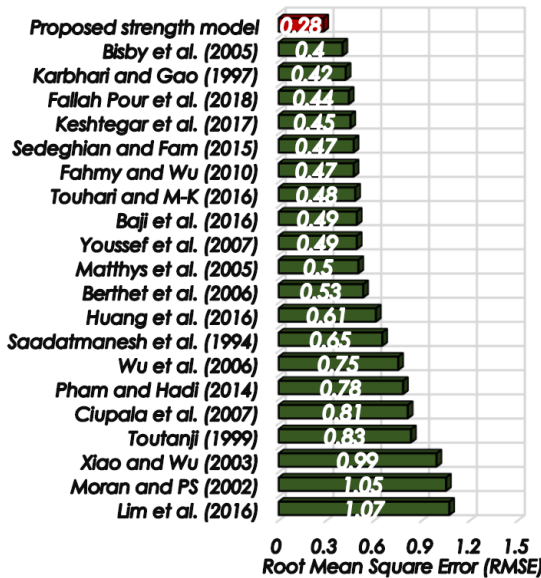


Fig. 6(b) Comparison of root mean square error (RMSE) of the proposed and existing strength models

6.3 Proposed strain model

Using the same procedure as in the proposed strength model, the strain ratio (ρ_ϵ), the stiffness ratio (ρ_K), and the volumetric ratio of the FRP (ρ_f) are found to be the most influencing parameters on the strain effectiveness of GFRP-wrapped concrete. Considering the effect of these parameters, a regression analysis was conducted on the experimental test database to find the best-fit equation. This resulted in the relationship shown in Eq. (15)

$$\frac{\epsilon_{cc}}{\epsilon_{co}} = \frac{3.57\rho_K\rho_\epsilon}{0.0842 + \rho_f} + \frac{2.31}{0.31\rho_\epsilon^2 - \rho_K} \quad (15)$$

This relationship can be written as some of the existing strain models (e.g., Karbhari and Gao 1997, Matthys *et al.*

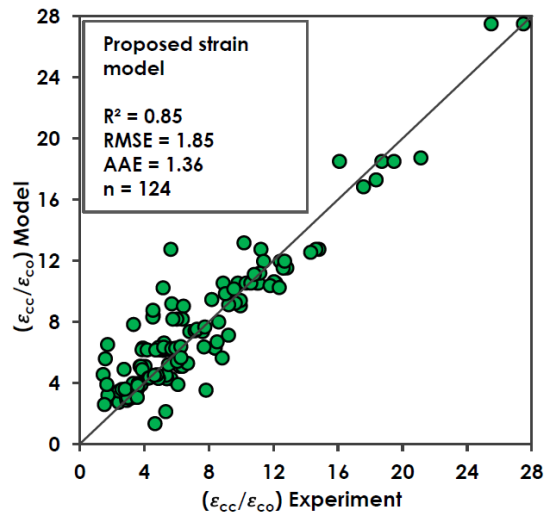


Fig. 7 Performance of the proposed strain model

2005, Saadatmanesh *et al.* 1994, Youssef *et al.* 2007) that used the general form of the expression proposed by Richart *et al.* (1928) for the ultimate strain (Eq. (16))

$$\frac{\epsilon_{cc}}{\epsilon_{co}} = c_2 + k_2 \frac{f_l}{f'_{co}} \quad (16)$$

Where, (c_2) is a calibration constant, and (k_2) is a strain enhancement coefficient. Large variety of strain equations that used a wide range of parameters have been proposed in the literature (e.g., Berthet *et al.* 2006, Fallah Pour *et al.* 2018, Lim *et al.* 2016, Xiao and Wu 2003). This can be attributed to the variability in the recorded experimental strains. For the proposed strain model, the equation of Richart *et al.* (1928) have been adopted and modified, where (k_2) was expressed as a function of the volumetric ratio (ρ_f), whereas (k_2) was expressed as a function the strain ratio (ρ_ϵ) and the stiffness ratio (ρ_K) as expressed in Eq. (17)

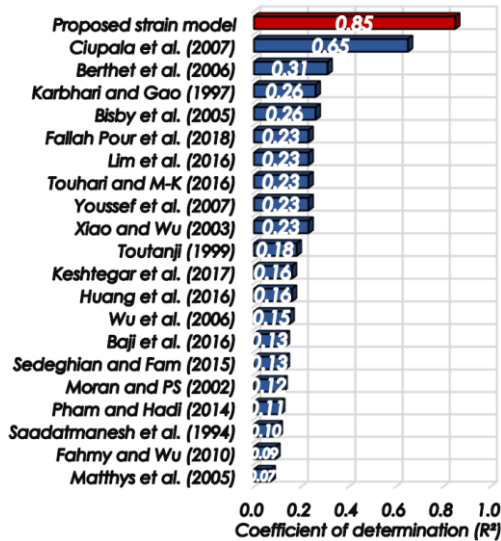


Fig. 8(a) Comparison of coefficient of determination (R²) of the proposed and existing strain models

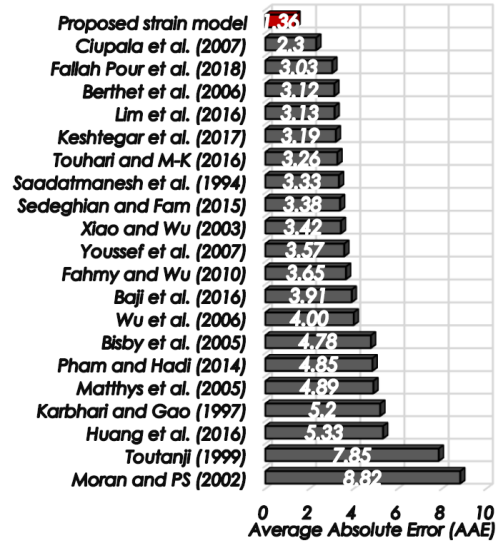


Fig. 8(c) Comparison of average absolute error (AAE) of the proposed and existing strain models

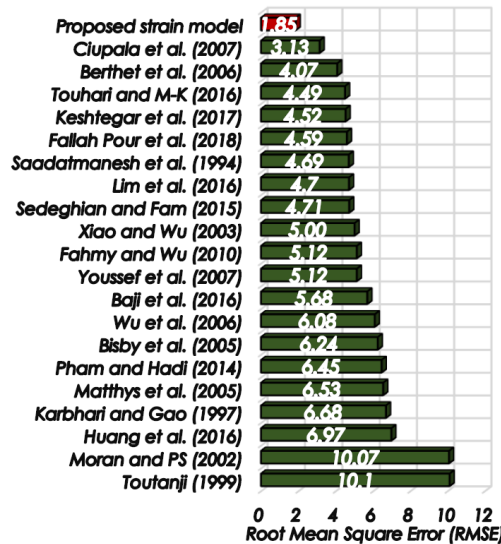


Fig. 8(b) Comparison of root mean square error (RMSE) of the proposed and existing strain models

$$\frac{\epsilon_{cc}}{\epsilon_{co}} = \left(\frac{3.57}{0.0842 + \rho_f} \right) \frac{f_{l,rup}}{f'_{co}} + \frac{2.31}{0.31 \rho_\epsilon^2 - \rho_K} \quad (17)$$

The performance of the proposed model is illustrated in Fig. 7. Good fit of the experimental data is observed with (R² = 0.85), and small indices of errors (RMSE = 1.85, and AAE = 1.36) showing high accuracy and low scatter of the data around the (45°) line.

6.4 Validation of the proposed strain model

Figs. 8(a)-(c) illustrate comparison of the statistical indices (R², RMSE, and AAE) of the proposed strain model and the 20 selected strain models. As shown by the figure, the proposed model outperformed the assessed models by a significant margin. It provides better fit of the experimental data with (R² = 0.85) compared to the others models, where the closest model of Ciupala et al. (2007) offered

(R² = 0.65). It is clear from Figs. 8(b)-(c) that the proposed model reveals very accurate predictions over the considered models showing the minimum errors (RMSE = 1.85, and AAE = 1.36), where the best accurate model of Ciupala et al. (2007) showed (RMSE = 3.13, and AAE = 2.3). Hence, it can be deduced that the proposed strain model is more efficient in predicting the ultimate strain of GFRP-wrapped concrete.

7. Conclusions

This paper has investigated 20 most used and recent design-oriented models for the prediction of the ultimate condition of GFRP-wrapped concrete. The models were reviewed and their applicability was assessed using a database of 163 experimental results of concrete cylinder confined with GFRP wraps. New design-oriented strength and strain models for concrete confined with GFRP wraps were proposed using regression analysis and compared to the existing models. Findings from this study can be summarized as follows:

- The predictions of the ultimate strain show much larger errors than those of the ultimate stress. This can be attributed to the scatter in the recorded experimental strains comparing to the experimental strengths.
- Of the 20 assessed models, those of Bisby et al. (2005), Fahmy and Wu (2010), and Fallah Pour et al. (2018) are the most accurate for the prediction of the ultimate strength. However, those of Berthet et al. (2006), Ciupala et al. (2007), and Touhari and Mitche-Kettab (2016) are the most accurate for the prediction of the ultimate strain.
- The proposed models provide accurate predictions and show significantly better performance over the existing models, particularly for ultimate strains. Such improved models applied for concrete strengths up to 128 MPa can be considered as useful tools for the future design applications.

References

- Ahmad, S.H., Khaloot, A.R. and Irshaid, A. (1991), "Behaviour of concrete spirally confined by fibreglass filaments", *Mag. Concrete Res.*, **43**(156), 143-148. <https://doi.org/10.1680/mac.1991.43.156.143>.
- Al Abadi, H., Abo El-Naga, H., Shaia, H. and Paton-Cole, V. (2016), "Refined approach for modelling strength enhancement of FRP-confined concrete", *Constr. Build. Mater.*, **119**, 152-174. <https://doi.org/10.1016/j.conbuildmat.2016.04.119>.
- Almusallam, T.H. (2007), "Behavior of normal and high-strength concrete cylinders confined with E-glass/epoxy composite laminates", *Compos. Part B: Eng.*, **38**(5-6), 629-639. <https://doi.org/10.1016/j.compositesb.2006.06.021>.
- Arabshahi, A., Gharaei-Moghaddam, N. and Tavakkolizadeh, M. (2020), "Development of applicable design models for concrete columns confined with aramid fiber reinforced polymer using Multi-Expression Programming", *Struct.*, **23**, 225-244. <https://doi.org/10.1016/j.istruc.2019.09.019>.
- Au, C. and Buyukozturk, O. (2005), "Effect of fiber orientation and ply mix on fiber reinforced polymer-confined concrete", *J. Compos. Constr.*, **9**(5), 397-407. [https://doi.org/10.1061/\(ASCE\)1090-0268\(2005\)9:5\(397\)](https://doi.org/10.1061/(ASCE)1090-0268(2005)9:5(397)).
- Baji, H., Ronagh, H.R. and Li, C.Q. (2016), "Probabilistic design models for ultimate strength and strain of FRP-confined concrete", *J. Compos. Constr.*, **20**(6), 04016051. [https://doi.org/10.1061/\(ASCE\)CC.1943-5614.0000704](https://doi.org/10.1061/(ASCE)CC.1943-5614.0000704).
- Bakshi, M., Abdollahi, B., Motavalli, M., Shekarchizade, M. and Gualibafian, M. (2007), "The experimental modeling of GFRP confined concrete cylinders subjected to axial loads", *Proceedings of the 8th International Symposium on Fiber Reinforced Polymer Reinforcement for Concrete Structures*, Patras, Greece, July.
- Bakis, C.E., Bank, L.C., Brown, V.L., Cosenza, E., Davalos, J.F., Lesko, J.J. and Triantafyllou, T.C. (2002), "Fiber-reinforced polymer composites for construction-State-of-the-Art review", *J. Compos. Constr.*, **6**(2), 73-87. [https://doi.org/10.1061/\(ASCE\)1090-0268\(2002\)6:2\(73\)](https://doi.org/10.1061/(ASCE)1090-0268(2002)6:2(73)).
- Benzaïd, R., Chikh, N. and Mesbah, H. (2009), "Study of the compressive behavior of short concrete columns confined by fiber reinforced composite", *Arab. J. Sci. Eng.*, **34**, 15-26.
- Berthet, J.F., Ferrier, E. and Hamelin, P. (2006), "Compressive behavior of concrete externally confined by composite jackets: Part B: modeling", *Constr. Build. Mater.*, **20**(5), 338-347. <https://doi.org/10.1016/j.conbuildmat.2005.01.029>.
- Bisby, L.A., Dent, A.J.S. and Green, M.F. (2005), "Comparison of confinement models for fiber-reinforced polymer-wrapped concrete", *ACI Struct. J.*, **102**(1), 62-72. <https://doi.org/10.14359/13531>.
- Cascardi, A., Micelli, F. and Aiello, M.A. (2017), "An Artificial Neural Networks model for the prediction of the compressive strength of FRP-confined concrete circular columns", *Eng. Struct.*, **140**, 199-208. <https://doi.org/10.1016/j.engstruct.2017.02.047>.
- Ciupala, M.A., Pilakoutas, K. and Mortazavi, A.A. (2007), "Effectiveness of FRP composites in confined concrete", *Proceedings of the 8th International Symposium on Fiber Reinforced Polymer Reinforcement for Concrete Structures*, Patras, Greece, July.
- Comert, M., Goksu, C. and Ilki, A. (2010), "Towards a tailored stress-strain behavior for FRP confined low strength concrete", *Third International Fib Congress Incorporating the PCI Annual Convention and Bridge Conference*, Washington, DC, USA, May-June.
- Cui, C. and Sheikh, S.A. (2010), "Experimental study of normal- and high-strength concrete confined with fiber-reinforced polymers", *J. Compos. Constr.*, **14**(5), 553-561. [https://doi.org/10.1061/\(asce\)cc.1943-5614.0000116](https://doi.org/10.1061/(asce)cc.1943-5614.0000116).
- Dai, J.G., Bai, Y.L. and Teng, J.G. (2011), "Behavior and modeling of concrete confined with FRP composites of large deformability", *J. Compos. Constr.*, **15**(6), 963-973. [https://doi.org/10.1061/\(ASCE\)CC.1943-5614.0000230](https://doi.org/10.1061/(ASCE)CC.1943-5614.0000230).
- De Lorenzis, L. and Tepfers, R. (2003), "Comparative study of models on confinement of concrete cylinders with fiber-reinforced polymer composites", *J. Compos. Constr.*, **7**(3), 219-237. [https://doi.org/10.1061/\(asce\)1090-0268\(2003\)7:3\(219\)](https://doi.org/10.1061/(asce)1090-0268(2003)7:3(219)).
- Ding, M., Chen, X., Zhang, X., Liu, Z. and Lu, J. (2018), "Study on seismic strengthening of railway bridge pier with CFRP and concrete jackets", *Earthq. Struct.*, **15**(3), 275-283. <https://doi.org/10.12989/eas.2018.15.3.275>.
- Djafar-Henni, I. and Kassoul, A. (2018), "Stress-strain model of confined concrete with Aramid FRP wraps", *Constr. Build. Mater.*, **186**, 1016-1030. <https://doi.org/10.1016/j.conbuildmat.2018.08.013>.
- Elwan, S.K. and Omar, M.A. (2014), "Experimental behavior of eccentrically loaded RC slender columns strengthened using GFRP wrapping", *Steel Compos. Struct.*, **17**(3), 271-285. <https://doi.org/10.12989/scs.2014.17.3.271>.
- Fahmy, M.F.M. and Wu, Z. (2010), "Evaluating and proposing models of circular concrete columns confined with different FRP composites", *Compos. Part B: Eng.*, **41**(3), 199-213. <https://doi.org/10.1016/j.compositesb.2009.12.001>.
- Faella, C., Realfonzo, R. and Salerno, N. (2005), "R/C elements confined by FRP", *Seismic Engineering for Concrete Structures - Italian Perspective, ACI Spring Convention*, New York City, USA, April.
- Fallah Pour, A., Ozbakkaloglu, T. and Vincent, T. (2018), "Simplified design-oriented axial stress-strain model for FRP-confined normal- and high-strength concrete", *Eng. Struct.*, **175**, 501-516. <https://doi.org/10.1016/j.engstruct.2018.07.099>.
- Fardis, M.N. and Khalili, H. (1981), "Concrete encased in fiberglass-fiber-reinforced plastic", *ACI J Proc.*, **78**(6), 440-6. doi:10.14359/10527.
- Fardis, M.N. and Khalili, H. (1982), "FRP-encased concrete as a structural material", *Mag. Concrete Res.*, **34**(121), 191-202. <https://doi.org/10.1680/mac.1982.34.121.191>.
- Green, M.F., Bisby, L.A., Fam, A.Z. and Kodur, V.K.R. (2006), "FRP confined concrete columns: Behaviour under extreme conditions", *Cement Concrete Compos.*, **28**(10), 928-937. <https://doi.org/10.1016/j.cemconcomp.2006.07.008>.
- Harries, K.A. and Carey, S.A. (2003), "Shape and 'gap' effects on the behavior of variably confined concrete", *Cement Concrete Res.*, **33**(6), 881-890. [https://doi.org/10.1016/S0008-8846\(02\)01085-2](https://doi.org/10.1016/S0008-8846(02)01085-2).
- Harries, K.A. and Kharel, G. (2002), "Behavior and modeling of concrete subject to variable confining pressure", *ACI Mater. J.*, **99**(2), 180-189.
- Hou, D., Wu, Z., Zheng, J. and Cui, Y. (2015), "Seismic rehabilitation of substandard RC columns with partially deteriorated concrete using CFRP composites", *Comput. Concrete*, **15**(1), 1-20. <https://doi.org/10.12989/cac.2015.15.1.001>.
- Huang, L., Gao, C., Yan, L., Kasal, B., Ma, G. and Tan, H. (2016), "Confinement models of GFRP-confined concrete: Statistical analysis and unified stress-strain models", *J. Reinf. Plast. Compos.*, **35**(11), 867-891. <https://doi.org/10.1177/0731684416630609>.
- Ilki, A., Kumbasar, N. and Koc, V. (2004), "Low strength concrete members externally confined with FRP sheets", *Struct. Eng. Mech.*, **18**(2), 167-194. <https://doi.org/10.12989/sem.2004.18.2.167>.
- Jiang, T. and Teng, J.G. (2007), "Analysis-oriented stress-strain models for FRP-confined concrete", *Eng. Struct.*, **29**(11), 2968-2986. <https://doi.org/10.1016/j.engstruct.2007.01.010>.
- Karbhari, V.M. and Gao, Y. (1997), "Composite jacketed concrete under uniaxial compression-verification of simple design equations", *J. Mater. Civil Eng.*, **9**(4), 185-193.

- [https://doi.org/10.1061/\(ASCE\)0899-1561\(1997\)9:4\(185\)](https://doi.org/10.1061/(ASCE)0899-1561(1997)9:4(185)).
- Keshtegar, B., Ozbakkaloglu, T. and Gholampour, A. (2017), "Modeling the behavior of FRP-confined concrete using dynamic harmony search algorithm", *Eng. Comput.*, **33**(3), 415-430. <https://doi.org/10.1007/s00366-016-0481-y>.
- Li, L.J., Xu, S.D., Zeng, L. and Guo, Y.C. (2013), "Compressive behavior of hybrid FRP confined concrete columns", *The 2013 World Congress on Advances in Structural Engineering and Mechanics (ASEM13)*, Jeju, Korea, September.
- Lam, L. and Teng, J.G. (2003), "Design-oriented stress-strain model for FRP-confined concrete", *Constr. Build. Mater.*, **17**(6-7), 471-489. [https://doi.org/10.1016/S0950-0618\(03\)00045-X](https://doi.org/10.1016/S0950-0618(03)00045-X).
- Lam, L. and Teng, J.G. (2004), "Ultimate condition of fiber reinforced polymer-confined concrete", *J. Compos. Constr.*, **8**(6), 539-548. [https://doi.org/10.1061/\(asce\)1090-0268\(2004\)8:6\(539\)](https://doi.org/10.1061/(asce)1090-0268(2004)8:6(539)).
- Li, G., Maricherla, D., Singh, K., Pang, S.S. and John, M. (2006), "Effect of fiber orientation on the structural behavior of FRP wrapped concrete cylinders", *Compos. Struct.*, **74**(4), 475-483. <https://doi.org/10.1016/J.COMPSTRUCT.2005.05.001>.
- Lim, J.C., Karakus, M. and Ozbakkaloglu, T. (2016), "Evaluation of ultimate conditions of FRP-confined concrete columns using genetic programming", *Comput. Struct.*, **162**, 28-37. <https://doi.org/10.1016/J.COMPSTRUCT.2015.09.005>.
- Lim, J.C. and Ozbakkaloglu, T. (2015), "Investigation of the influence of the application path of confining pressure: Tests on actively confined and FRP-confined concretes", *J. Struct. Eng.*, **141**(8), 04014203. [https://doi.org/10.1061/\(ASCE\)ST.1943-541X.0001177](https://doi.org/10.1061/(ASCE)ST.1943-541X.0001177).
- Lim, J.C. and Ozbakkaloglu, T. (2015), "Confinement model for FRP-confined high-strength concrete", *J. Compos. Constr.*, **18**(4). [https://doi.org/10.1061/\(ASCE\)CC.1943-5614.0000376](https://doi.org/10.1061/(ASCE)CC.1943-5614.0000376).
- Lin, H.J. and Chen, C.T. (2001), "Strength of concrete cylinder confined by composite materials", *J. Reinf. Plast. Compos.*, **20**(18), 1577-1600. <https://doi.org/10.1177/073168401772679066>.
- Lin, H.J. and Liao, C.I. (2004), "Compressive strength of reinforced concrete column confined by composite material", *Compos. Struct.*, **65**(2), 239-250. <https://doi.org/10.1016/J.COMPSTRUCT.2003.11.001>.
- Mandal, S., Hoskin, A. and Fam, A. (2005), "Influence of concrete strength on confinement effectiveness of fiber-reinforced polymer circular jackets", *ACI Struct. J.*, **102**(3), 383-392. <https://doi.org/10.14359/14409>.
- Mander, J.B., Priestley, M.J.N. and Park, R. (1988), "Theoretical stress-strain model for confined concrete", *J. Struct. Eng.*, **114**(8), 1804-26. [https://doi.org/10.1061/\(ASCE\)0733-9445\(1988\)114:8\(1804\)](https://doi.org/10.1061/(ASCE)0733-9445(1988)114:8(1804)).
- Mastrapa, J. (1997), "Effect of construction bond on confinement with fiber composites", Masters Thesis, University of Central Florida, Florida, USA.
- Matthys, S., Toutanji, H., Audenaert, K. and Taerwe, L. (2005), "Axial load behavior of large-scale columns confined with fiber-reinforced polymer composites", *ACI Struct. J.*, **102**(2), 258-267. <https://doi.org/10.14359/14277>.
- Mesbah, H.A. and Benzaid, R. (2017), "Damage-based stress-strain model of RC cylinders wrapped with CFRP composites", *Adv. Concrete Constr.*, **5**(5), 539-561. <https://doi.org/10.12989/acc.2017.5.5.539>.
- Micelli, F. and Modarelli, R. (2013), "Experimental and analytical study on properties affecting the behaviour of FRP-confined concrete", *Compos. Part B: Eng.*, **45**(1), 1420-1431. <https://doi.org/10.1016/J.COMPOSITESB.2012.09.055>.
- Mirmiran, A., Kargahi, M., Samaan, M.S. and Shahawy, M. (1996), "Composite FRP-concrete column with bi-directional external reinforcement", *Proceedings of the 1st International Conference in Composites in Infrastructure*, Arizona, USA.
- Miyuchi, K., Nishibayashi, S. and Inoue, S. (1997), "Estimation of strengthening effects with carbon fiber sheet for concrete column", *Int. Symp. 3rd, Non-metallic Reinf. Concr. Struct.*, Sapporo, Japan.
- Moran, D.A. and Pantelides, C.P. (2002), "Variable strain ductility ratio for fiber-reinforced polymer-confined concrete", *J. Compos. Constr.*, **6**(4), 224-232. [https://doi.org/10.1061/\(asce\)1090-0268\(2002\)6:4\(224\)](https://doi.org/10.1061/(asce)1090-0268(2002)6:4(224)).
- Nanni, A. and Bradford, N.M. (1995), "FRP jacketed concrete under uniaxial compression", *Constr. Build. Mater.*, **9**(2), 115-124. [https://doi.org/10.1016/0950-0618\(95\)00004-Y](https://doi.org/10.1016/0950-0618(95)00004-Y).
- Newman, K. and Newman, J.B. (1972), "Failure theories and design criteria for plain concrete". *Structure, Solid Mechanics and Engineering Design: The Proceedings, International Association of Testing and Research Laboratories for Materials and Structures*, London.
- Ozbakkaloglu, T. and Akin, E. (2012), "Behavior of FRP-confined normal- and high-strength concrete under cyclic axial compression", *J. Compos. Constr.*, **16**(4), 451-463. [https://doi.org/10.1061/\(ASCE\)CC.1943-5614.0000273](https://doi.org/10.1061/(ASCE)CC.1943-5614.0000273).
- Ozbakkaloglu, T., Lim, J.C. and Vincent, T. (2013), "FRP-confined concrete in circular sections: Review and assessment of stress-strain models", *Eng. Struct.*, **49**, 1068-1088. <https://doi.org/10.1016/j.engstruct.2012.06.010>.
- Pessiki, S., Harries, K.A., Kestner, J.T., Sause, R. and Ricles, J.M. (2001), "Axial behavior of reinforced concrete columns confined with FRP jackets", *J. Compos. Constr.*, **5**(4), 237-245. [https://doi.org/10.1061/\(ASCE\)1090-0268\(2001\)5:4\(237\)](https://doi.org/10.1061/(ASCE)1090-0268(2001)5:4(237)).
- Pham, T.M. and Hadi, M.N.S. (2014), "Confinement model for FRP confined normal- and high-strength concrete circular columns", *Constr. Build. Mater.*, **69**, 83-90. <https://doi.org/10.1016/J.CONBUILDMAT.2014.06.036>.
- Rashid, R.S.M. and Aboutaha, R.S. (2014), "Analytical model for CFRP strengthened circular RC column under elevated temperature", *Comput. Concrete*, **13**(4), 517-529. <https://doi.org/10.12989/cac.2014.13.4.517>.
- Richart, F., Brandtzaeg, A. and Brown, R.L. (1928), "A study of the failure of concrete under combined compressive stresses". University of Illinois Bulletin, **26**(12), University of Illinois at Urbana Champaign, USA.
- Saadatmanesh, H., Ehsani, M.R. and Li, M.W. (1994), "Strength and ductility of concrete columns externally reinforced with fiber composite straps", *ACI Struct. J.*, **91**(4), 434-447.
- Saafi, M., Toutanji, H. and Li, Z. (1999), "Behavior of concrete columns confined with fiber reinforced polymer tubes", *ACI Mater. J.*, **96**(4), 500-509. <https://doi.org/10.14359/652>.
- Sadeghian, P. and Fam, A. (2015), "Improved design-oriented confinement models for FRP-wrapped concrete cylinders based on statistical analyses", *Eng. Struct.*, **87**, 162-182. <https://doi.org/10.1016/J.ENGSTRUCT.2015.01.024>.
- Samaan, M., Mirmiran, A. and Shahawy, M. (1998), "Model of concrete confined by fiber composites", *J. Struct. Eng.*, **124**(9), 1025-1031. [https://doi.org/10.1061/\(ASCE\)0733-9445\(1998\)124:9\(1025\)](https://doi.org/10.1061/(ASCE)0733-9445(1998)124:9(1025)).
- Schmidt, M. and Lipson, H. (2009), "Distilling free-form natural laws from experimental data", *Sci.*, **324**(5923), 81-85. <https://doi.org/10.1126/science.1165893>.
- Shahawy, M., Mirmiran, A. and Beitelman, T. (2000), "Tests and modeling of carbon-wrapped concrete columns", *Compos. Part B: Eng.*, **31**(6-7), 471-480. [https://doi.org/10.1016/S1359-8368\(00\)00021-4](https://doi.org/10.1016/S1359-8368(00)00021-4).
- Shao, Y., Zhu, Z. and Mirmiran, A. (2006), "Cyclic modeling of FRP-confined concrete with improved ductility", *Cement Concrete Compos.*, **28**(10), 959-968. <https://doi.org/10.1016/J.CEMCONCOMP.2006.07.009>.
- Shehata, I.A.E.M., Carneiro, L.A.V. and Shehata, L.C.D. (2002), "Strength of short concrete columns confined with CFRP sheets", *Mater. Struct.*, **35**(1), 50-58. <https://doi.org/10.1007/BF02482090>.

- Silva, M.A. and Rodrigues, C.C. (2006), "Size and relative stiffness effects on compressive failure of concrete columns wrapped with glass FRP", *J. Mater. Civil Eng.*, **18**(3), 334-342. [https://doi.org/10.1061/\(ASCE\)0899-1561\(2006\)18:3\(334\)](https://doi.org/10.1061/(ASCE)0899-1561(2006)18:3(334)).
- Sonnenschein, R., Gajdosova, K. and Holly, I. (2016), "FRP composites and their using in the construction of bridges", *Procedia Eng.*, **161**, 477-482. <https://doi.org/10.1016/j.proeng.2016.08.665>.
- Spoelstra, M.R. and Monti, G. (1999), "FRP-confined concrete model", *J. Compos. Constr.*, **3**(3), 143-150. [https://doi.org/10.1061/\(ASCE\)1090-0268\(1999\)3:3\(143\)](https://doi.org/10.1061/(ASCE)1090-0268(1999)3:3(143)).
- Sumathi, A. and Vignesh, S.A. (2017), "Study on behavior of RCC beams with externally bonded FRP members in flexure", *Adv. Concrete Constr.*, **5**(6), 625-638. <https://doi.org/10.12989/acc.2017.5.6.625>.
- Touhari, M. and Mitiche-Kettab, R. (2016), "Behaviour of FRP confined concrete cylinders: Experimental investigation and strength model", *Periodica Polytechnica Civil Eng.*, **60**(4), 647-660. <https://doi.org/10.3311/PPci.8759>.
- Toutanji, H. (1999), "Stress-strain characteristics of concrete columns externally confined with advanced fiber composite sheets", *ACI Mater. J.*, **96**(3), 397-404. <https://doi.org/10.14359/639>.
- Vincent, T. and Ozbakkaloglu, T. (2013), "Influence of concrete strength and confinement method on axial compressive behavior of FRP confined high- and ultra high-strength concrete", *Compos. Part B: Eng.*, **50**, 413-428. <https://doi.org/10.1016/j.compositesb.2013.02.017>.
- Wang, Y.F. and Wu, H.L. (2011), "Size effect of concrete short columns confined with aramid FRP jackets", *J. Compos. Constr.*, **15**(4), 535-544. [https://doi.org/10.1061/\(ASCE\)CC.1943-5614.0000178](https://doi.org/10.1061/(ASCE)CC.1943-5614.0000178).
- Wu, G., Lü, Z.T. and Wu, Z.S. (2006), "Strength and ductility of concrete cylinders confined with FRP composites", *Constr. Build. Mater.*, **20**(3), 134-148. <https://doi.org/10.1016/J.CONBUILDMAT.2005.01.022>.
- Wu, G., Wu, Z.S., Lu, Z.T. and Ando, Y.B. (2008), "Structural performance of concrete confined with hybrid FRP composites", *J. Reinf. Plast. Compos.*, **27**(12), 1323-1348. <https://doi.org/10.1177/0731684407084989>.
- Wu, H.L. and Wang, Y.F. (2010), "Experimental study on reinforced high-strength concrete short columns confined with AFRP sheets", *Steel Compos. Struct.*, **10**(6), 501-516. <https://doi.org/10.12989/scs.2010.10.6.501>.
- Wu, H.L., Wang, Y.F., Yu, L. and Li, X.R. (2009), "Experimental and computational studies on high-strength concrete circular columns confined by aramid fiber-reinforced polymer sheets", *J. Compos. Constr.*, **13**(2), 125-34. [https://doi.org/10.1061/\(ASCE\)1090-0268\(2009\)13:2\(125\)](https://doi.org/10.1061/(ASCE)1090-0268(2009)13:2(125)).
- Wu, Y.F., Xu, X.S., Sun, J.B. and Jiang, C. (2012), "Analytical solution for the bond strength of externally bonded reinforcement", *Compos. Struct.*, **94**(11), 3232-3239. <https://doi.org/10.1016/j.compstruct.2012.04.026>.
- Xiao, Y. and Wu, H. (2000), "Compressive behavior of concrete confined by carbon fiber composite jackets", *J. Mater. Civil Eng.*, **12**(2), 139-146. [https://doi.org/10.1061/\(ASCE\)0899-1561\(2000\)12:2\(139\)](https://doi.org/10.1061/(ASCE)0899-1561(2000)12:2(139)).
- Xiao, Y. and Wu, H. (2003), "Compressive behavior of concrete confined by various types of FRP composite jackets", *J. Reinf. Plast. Compos.*, **22**(13), 1187-1201. <https://doi.org/10.1177/0731684403035430>.
- Youssef, M.N., Feng, M.Q. and Mosallam, A.S. (2007), "Stress-strain model for concrete confined by FRP composites", *Compos. Part B: Eng.*, **38**(5-6), 614-628. <https://doi.org/10.1016/J.COMPOSITESB.2006.07.020>.

Appendix 1

Table 1 Summary of the test results

No.	Source	Specimen dimensions			Unconfined concrete properties		GFRP properties					Experimental results				
		d (mm)	h (mm)	h/d	f'_{co} (MPa)	ε_{co} (%)	E_f (GPa)	f_f (MPa)	t_f (mm)	ε_f (%)	f'_{cc} (MPa)	ε_{cc} (%)	$\varepsilon_{h,rup}$ (%)	k_ε	f'_{cc}/f'_{co}	$\varepsilon_{cc}/\varepsilon_{co}$
1	Ahmad <i>et al.</i> (1991)	101.6	203.2	2.00	38.99	0.20	48.3	2070	0.8	4.286	115.3	1.130		2.96	5.65	
2		101.6	203.2	2.00	50.51	0.24	48.3	2070	0.8	4.286	135.1	1.240		2.67	5.17	
3		101.6	203.2	2.00	64.2	0.27	48.3	2070	0.8	4.286	145.59	1.230		2.27	4.56	
4	Nanni and Bradford (1995)	150	300	2.00	36.3	0.28	52	175	0.3	0.337	46	2.292		1.27	8.19	
5		150	300	2.00	36.3	0.28	52	175	0.6	0.337	60.52	3.079		1.67	11.00	
6		150	300	2.00	36.3	0.28	52	175	0.6	0.337	59.23	3.405		1.63	12.16	
7		150	300	2.00	36.3	0.28	52	175	0.6	0.337	59.77	2.744		1.65	9.80	
8		150	300	2.00	36.3	0.28	52	175	0.6	0.337	60.16	2.887		1.66	10.31	
9		150	300	2.00	36.3	0.28	52	175	0.6	0.337	69.02	3.100		1.90	11.07	
10		150	300	2.00	36.3	0.28	52	175	0.6	0.337	55.75	2.489		1.54	8.89	
11		150	300	2.00	36.3	0.28	52	175	0.6	0.337	56.41	2.968		1.55	10.60	
12		150	300	2.00	36.3	0.28	52	175	1.2	0.337	84.88	3.145		2.34	11.23	
13		150	300	2.00	36.3	0.28	52	175	1.2	0.337	84.33	4.150		2.32	14.82	
14		150	300	2.00	36.3	0.28	52	175	1.2	0.337	79.64	4.100		2.19	14.64	
15		150	300	2.00	36.3	0.28	52	175	2.4	0.337	106.87	5.242		2.94	18.72	
16		150	300	2.00	36.3	0.28	52	175	2.4	0.337	104.94	5.453		2.89	19.48	
17		150	300	2.00	36.3	0.28	52	175	2.4	0.337	107.91	4.509		2.97	16.10	
18		Karbhari and Gao (1997)	152	305	2.01	18.01		35.856	513.1	5.31	1.431	82.25	2.400		4.57	
19		Mastrapa (1997)	152.5	305	2.00	31.2		11.703	345	3	2.948	64.67	2.950	2.223	0.770	2.07
20			152.5	305	2.00	31.2		11.703	345	3	2.948	64.7	3.150	1.972	0.680	2.07
21	152.5		305	2.00	31.2		11.703	345	5	2.948	91	3.800	1.798	0.620	2.92	
22	152.5		305	2.00	31.2		11.703	345	5	2.948	96.9	6.200	1.769	0.610	3.11	
23	152.5		305	2.00	31.2		11.703	345	3	2.948	63.1	2.650	2.204	0.760	2.02	
24	152.5		305	2.00	31.2		11.703	345	3	2.948	65.4	2.800	2.175	0.750	2.10	
25	152.5		305	2.00	31.2		11.703	345	5	2.948	91.9	4.200	1.943	0.670	2.95	
26	152.5		305	2.00	31.2		11.703	345	5	2.948	89	4.800	1.711	0.590	2.85	
27	Lin and Chen (2001)		120	240	2.00	32.7	0.20	32.9	743.9	0.9	2.261	62.2			1.90	
28		120	240	2.00	32.7	0.20	32.9	743.9	0.9	2.261	61.4			1.88		
29		120	240	2.00	32.7	0.20	32.9	743.9	0.9	2.261	66.3			2.03		
30		120	240	2.00	32.7	0.20	32.9	743.9	1.8	2.261	101.3			3.10		
31		120	240	2.00	32.7	0.20	32.9	743.9	1.8	2.261	88			2.69		
32		120	240	2.00	32.7	0.20	32.9	743.9	1.8	2.261	104.5			3.20		
33	Harries and Kharel (2002)	152	305	2.01	32.1	0.28	4.9*	75*	9*	1.531	46.7	0.680	1.110	0.725	1.45	2.43
34		152	305	2.01	32.1	0.28	4.9*	75*	12*	1.531	50.2	0.820	1.090	0.712	1.56	2.93
35		152	305	2.01	32.1	0.28	4.9*	75*	15*	1.531	60	0.870	1.110	0.725	1.87	3.11
36	Harries and Carey (2003)	152	305	2.01	32.1	0.39	4.9*	75*	9*	1.600	53.2	0.950	1.438	0.900	1.66	2.44
37		152	305	2.01	32.1	0.39	4.9*	75*	9*	1.600	46.7	0.680	1.132	0.900	1.45	1.74
38	Lin and Liao (2004)	100	200	2.00	26.987		23.8253	445.437	1.84	1.870	62.422			2.31		
39		100	200	2.00	20.888		23.8253	445.437	1.84	1.870	62.056			2.97		
40		100	200	2.00	23.846		23.8253	445.437	1.84	1.870	61.446			2.58		
41		100	200	2.00	26.987		22.4579	403.141	3.89	1.795	93.557			3.47		
42		100	200	2.00	20.888		22.4579	403.141	3.89	1.795	90.69			4.34		
43		100	200	2.00	23.846		22.4579	403.141	3.89	1.795	88.983			3.73		
44		Lam and Teng (2004)	152	305	2.01	38.5		22.455	490	1.27	2.325	56.2		1.849	0.744	1.46
45			152	305	2.01	38.5		22.455	490	1.27	2.325	51.9	1.315	1.442	0.744	1.35
46			152	305	2.01	38.5		22.455	490	1.27	2.325	58.3	1.459	1.885	0.744	1.51
47	152		305	2.01	38.5		22.455	490	2.54	2.325	75.7	2.457	1.762	0.744	1.97	
48	152		305	2.01	38.5		22.455	490	2.54	2.325	77.3	2.188	1.674	0.744	2.01	
49	152		305	2.01	38.5		22.455	490	2.54	2.325	75.2		1.772	0.744	1.95	

Table 1 Continued

No.	Source	Specimen dimensions			Unconfined concrete properties		GFRP properties				Experimental results					
		d (mm)	h (mm)	h/d	f'_{co} (MPa)	ϵ_{co} (%)	E_f (GPa)	f_f (MPa)	t_f (mm)	ϵ_f (%)	f'_{cc} (MPa)	ϵ_{cc} (%)	$\epsilon_{h,rupt}$ (%)	k_c	f'_{cc}/f'_{co}	$\epsilon_{cc}/\epsilon_{co}$
50		150	300	2.00	35		80.7	2560	0.48	3.500	60	0.943	1.200	0.343	1.71	
51		150	300	2.00	35		80.7	2560	0.48	3.500	59.4	1.637	1.683	0.481	1.70	
52		150	300	2.00	35		80.7	2560	0.48	3.500	61.2	0.930	1.371	0.392	1.75	
53	Faella <i>et al.</i> (2005)	150	300	2.00	35		80.7	2560	0.48	3.500	61.7				1.76	
54		150	300	2.00	35		80.7	2560	0.96	3.500	76.3	1.190	1.061	0.303	2.18	
55		150	300	2.00	35		80.7	2560	0.96	3.500	86.1	1.056	1.047	0.299	2.46	
56		150	300	2.00	35		80.7	2560	0.96	3.500	78.6				2.25	
57		150	300	2.00	35		80.7	2560	0.96	3.500	84.6				2.42	
58		100	200	2.00	30.7	0.27	26.1	575	1.3	2.200	54.5	1.540			1.78	5.70
59		100	200	2.00	30.7	0.27	26.1	575	2.6	2.200	79.3	2.750			2.58	10.19
60		100	200	2.00	46.3	0.23	26.1	575	1.3	2.200	58.5	0.900			1.26	3.91
61	Mandal <i>et al.</i> (2005)	100	200	2.00	46.3	0.23	26.1	575	2.6	2.200	83.8	1.480			1.81	6.43
62		100	200	2.00	54.5	0.24	26.1	575	2.6	2.200	84.1	0.800			1.54	3.33
63		100	200	2.00	67.1	0.22	26.1	575	1.3	2.200	86.8	0.320			1.29	1.45
64		100	200	2.00	67.1	0.22	26.1	575	2.6	2.200	95	0.380			1.42	1.73
65		100	200	2.00	80.6	0.22	26.1	575	1.3	2.200	102.7	0.370			1.27	1.68
66		100	200	2.00	80.6	0.22	26.1	575	2.6	2.200	98.3	0.350			1.22	1.59
67	Au and Buyukozturk (2005)	150	375	2.50	24.2	0.36	26.1	575	1.2	2.200	43.8	1.630	1.480	0.672	1.81	4.53
68	Li <i>et al.</i> (2006)	152.4	304.8	2.00	45.6	0.80	15.1	320.2	1.476	2.320	54.62	2.200			1.20	2.75
69	Green <i>et al.</i> (2006)	152	305	2.01	59		33.8*	748*	2*	2.200	73				1.24	
70	Shao <i>et al.</i> (2006)	152	305	2.01	40.2	0.22	26.13	610	1.02	2.500	49.6	0.730	1.340		1.23	3.32
71		152	305	2.01	40.2	0.22	26.13	610	2.03	2.500	71.4	0.850	1.320		1.78	3.86
72		150	300	2.00	31.1	0.21	21.3	575	2.54	2.700	91.6	2.610	2.180		2.95	12.43
73		150	300	2.00	29.6	0.19	21.3	575	2.54	2.700	89.4	2.720	2.180		3.02	14.32
74	Silva and Rodrigues (2006)	150	300	2.00	31.1	0.20	21.3	575	2.54	2.700	87.5	2.280	2.180		2.81	11.40
75		150	450	3.00	31.1		21.3	575	2.54	2.700	91.9	2.340	2.180		2.95	
76		150	450	3.00	29.6		21.3	575	2.54	2.700	89.8	2.320	2.180		3.03	
77		150	450	3.00	31.2		21.3	575	2.54	2.700	91.9	2.310	2.180		2.95	
78		250	750	3.00	31.2	0.24	21.3	575	2.54	2.700	55.8	1.090	2.180		1.79	4.54
79		406.4	812.8	2.00	29.4	0.24	18.5	425	7.267	2.160	70.77	1.527			2.41	6.36
80		406.4	812.8	2.00	29.4	0.24	18.5	425	7.267	2.160	71.78	1.445			2.44	6.02
81		406.4	812.8	2.00	29.4	0.24	18.5	425	7.267	2.160	76.78	1.387			2.61	5.78
82		406.4	812.8	2.00	29.4	0.24	18.5	425	4.472	2.160	49.53	1.345			1.68	5.60
83		406.4	812.8	2.00	29.4	0.24	18.5	425	4.472	2.160	54.9	1.003			1.87	4.18
84		406.4	812.8	2.00	29.4	0.24	18.5	425	4.472	2.160	61.19	1.189			2.08	4.95
85		406.4	812.8	2.00	29.4	0.24	18.5	425	3.354	2.160	49.3	0.971			1.68	4.05
86		406.4	812.8	2.00	29.4	0.24	18.5	425	3.354	2.160	51.19	0.897			1.74	3.74
87		406.4	812.8	2.00	29.4	0.24	18.5	425	3.354	2.160	47.88	0.912			1.63	3.80
88	Youssef <i>et al.</i> (2007)	406.4	812.8	2.00	29.4	0.24	18.5	425	1.677	2.160	44.14	0.781			1.50	3.25
89		406.4	812.8	2.00	29.4	0.24	18.5	425	1.677	2.160	42.96	0.695			1.46	2.90
90		406.4	812.8	2.00	29.4	0.24	18.5	425	1.677	2.160	45.11	0.715			1.53	2.98
91		152.4	304.8	2.00	44.1	0.24	18.5	425	3.354	2.160	94.1	2.013			2.13	8.39
92		152.4	304.8	2.00	44.1	0.24	18.5	425	3.354	2.160	91.87	2.014			2.08	8.39
93		152.4	304.8	2.00	44.1	0.24	18.5	425	3.354	2.160	89.29	2.011			2.02	8.38
94		152.4	304.8	2.00	44.1	0.24	18.5	425	2.236	2.160	80.39	1.518			1.82	6.33
95		152.4	304.8	2.00	44.1	0.24	18.5	425	2.236	2.160	80.04	1.488			1.81	6.20
96		152.4	304.8	2.00	44.1	0.24	18.5	425	2.236	2.160	81.13	1.530			1.84	6.38
97		152.4	304.8	2.00	44.1	0.24	18.5	425	1.677	2.160	66.2	1.298			1.50	5.41
98	152.4	304.8	2.00	44.1	0.24	18.5	425	1.677	2.160	66.6	1.357			1.51	5.65	
99	152.4	304.8	2.00	44.1	0.24	18.5	425	1.677	2.160	63.62	1.295			1.44	5.40	
100		150	300	2.00	47.72	0.31	27	540	3.9	2.000	100.11	2.723	0.800		2.10	8.83
101	Almusallam (2007)	150	300	2.00	50.57	0.29	27	540	3.9	2.000	89.88	1.968	0.802		1.78	6.68
102		150	300	2.00	60.52	0.30	27	540	3.9	2.000	99.6	1.597	0.698		1.65	5.37
103		150	300	2.00	80.82	0.27	27	540	3.9	2.000	101.43	0.694	0.869		1.26	2.62
104		150	300	2.00	90.29	0.32	27	540	3.9	2.000	110	0.900	0.825		1.22	2.81

Table 1 Continued

No.	Source	Specimen dimensions			Unconfined concrete properties		GFRP properties					Experimental results				
		<i>d</i> (mm)	<i>h</i> (mm)	<i>h/d</i>	<i>f_{co}</i> (MPa)	<i>ε_{co}</i> (%)	<i>E_f</i> (GPa)	<i>f_f</i> (MPa)	<i>t_f</i> (mm)	<i>ε_f</i> (%)	<i>f_{cc}</i> (MPa)	<i>ε_{cc}</i> (%)	<i>ε_{h,rip}</i> (%)	<i>k_c</i>	<i>f_{co}/f_{co}</i>	<i>ε_{co}/ε_{co}</i>
105	Bakhshi <i>et al.</i> (2007)	150	300	2.00	14.8	0.24	26.49	537	0.508	2.027	30	1.850			2.03	7.71
106		150	300	2.00	25.1	0.23	26.49	537	0.508	2.027	34.2	1.400			1.36	6.09
107		150	300	2.00	41.7	0.28	26.49	537	0.508	2.027	51.9	0.430			1.24	1.54
108		150	300	2.00	25.1	0.23	26.49	537	1.016	2.027	55.5	1.960			2.21	8.52
109		150	300	2.00	25.1	0.23	26.49	537	2.032	2.027	83.3	2.770			3.32	12.04
110	Wu <i>et al.</i> (2008)	150	300	2.00	23.1	0.27	73	1500	0.354	2.055	46.4	2.490			2.01	9.22
111		150	300	2.00	22.7	0.31	73	1500	0.354	2.055	45	2.360			1.98	7.61
112	Benzaid <i>et al.</i> (2009)	160	320	2.00	56.7	0.24	23.8	383	0.44	2.120	74	1.120	1.140	0.708	1.31	4.67
113		160	320	2.00	56.7	0.24	23.8	383	0.88	2.120	84	1.280	1.150	0.715	1.48	5.33
114		160	320	2.00	56.7	0.24	23.8	383	1.76	2.120	95.5	1.880	1.260	0.783	1.68	7.83
115	Comert <i>et al.</i> (2010)	150	300	2.00	9.3	0.20	65	1700	0.56	2.800	41	5.500			4.41	27.50
116		150	300	2.00	9.3	0.20	65	1700	0.56	2.800	43.2	5.100			4.65	25.50
117	Cui and Sheikh (2010)	152	305	2.01	47.76	0.22	26.84	620	1.25	2.310	59.1	1.350	2.020	0.874	1.24	6.08
118		152	305	2.01	47.76	0.22	26.84	620	1.25	2.310	59.8	1.150	2.143		1.25	5.18
119		152	305	2.01	47.76	0.22	26.84	620	2.5	2.310	88.9	2.210	2.032	0.880	1.86	9.95
120		152	305	2.01	47.76	0.22	26.84	620	2.5	2.310	88	2.210	2.114		1.84	9.95
121		152	305	2.01	47.76	0.22	26.84	620	3.75	2.310	113.2	2.850	2.112		2.37	12.84
122		152	305	2.01	47.76	0.22	26.84	620	3.75	2.310	112.5	2.800	2.110		2.36	12.61
123		152	305	2.01	47.76	0.22	26.84	620	1.25	2.310	63.4	1.150	2.179		1.33	5.18
124		152	305	2.01	47.76	0.22	26.84	620	1.25	2.310	62.4	1.350	2.116		1.31	6.08
125		152	305	2.01	47.76	0.22	26.84	620	2.5	2.310	89.7	2.140	2.074	0.898	1.88	9.64
126		152	305	2.01	47.76	0.22	26.84	620	2.5	2.310	88.3	2.050	2.049	0.887	1.85	9.23
127		152	305	2.01	47.76	0.22	26.84	620	3.75	2.310	108	2.620	1.893	0.819	2.26	11.80
128		152	305	2.01	79.9	0.24	26.84	620	3.75	2.310	120.8	1.260	2.008	0.869	1.51	5.23
129		152	305	2.01	79.9	0.24	26.84	620	3.75	2.310	126.1	1.180	1.916	0.829	1.58	4.90
130	152	305	2.01	110.6	0.26	26.84	620	5	2.310	174.6	0.950	1.398	0.605	1.58	3.63	
131	152	305	2.01	110.6	0.26	26.84	620	5	2.310	172.9	1.280	1.538	0.666	1.56	4.89	
132	Micelli and Modarelli (2013)	150	300	2.00	28.35	0.49	65	1700	0.23	2.600	53.27	1.900	4.980		1.88	3.88
133	Li <i>et al.</i> (2013)	150	300	2.00	31.72	0.30	69.45	1079	0.222	2.230	47.63	1.081	1.225	0.600	1.50	3.58
134	Lim and Ozbakkaloglu (2015)	63	126	2.00	51.6	0.25	95.3	3055	0.2	3.210	101.2	3.030	2.350	0.733	1.96	12.37
135		63	126	2.00	51.6	0.25	95.3	3055	0.4	3.210	153.7	4.310	2.190	0.683	2.98	17.59
136		63	126	2.00	51.6	0.25	95.3	3055	0.4	3.210	152.9	4.500	2.250	0.702	2.96	18.37
137		63	126	2.00	51.6	0.25	95.3	3055	0.4	3.210	174.7	5.180	2.440	0.761	3.39	21.14
138		63	126	2.00	128	0.32	95.3	3055	0.4	3.210	161.8	2.150	2.340	0.730	1.26	6.83
139	63	126	2.00	128	0.32	95.3	3055	0.4	3.210	166.3	2.250	2.360	0.736	1.30	7.14	
140	Touhari and Mitche-Kettab (2016)	160	320	2.00	26.2	0.27	26	325	1	1.900	38.3	1.500	1.480	0.780	1.46	5.62
141		160	320	2.00	26.2	0.27	26	325	1	1.900	34.6	1.260	1.450	0.760	1.32	4.72
142		160	320	2.00	26.2	0.27	26	325	1	1.900	38	1.390	1.500	0.790	1.45	5.21
143		160	320	2.00	26.2	0.27	26	325	2	1.900	49.4	2.410	1.450	0.760	1.89	9.03
144		160	320	2.00	26.2	0.27	26	325	2	1.900	52.5	2.550	1.500	0.790	2.00	9.55
145		160	320	2.00	26.2	0.27	26	325	3	1.900	62.8	3.390	1.400	0.740	2.40	12.70
146		160	320	2.00	26.2	0.27	26	325	3	1.900	56.4	2.980	1.300	0.680	2.15	11.16
147		160	320	2.00	26.2	0.27	26	325	3	1.900	54.7	2.890	1.290	0.680	2.09	10.82
148		160	320	2.00	42.6	0.29	26	325	1	1.900	56.5	1.100	1.430	0.750	1.33	3.81
149		160	320	2.00	42.6	0.29	26	325	1	1.900	55.5	1.040	1.400	0.730	1.30	3.60
150		160	320	2.00	42.6	0.29	26	325	1	1.900	59.8	1.230	1.630	0.860	1.40	4.26
151		160	320	2.00	42.6	0.29	26	325	2	1.900	68.5	1.650	1.460	0.770	1.61	5.71
152		160	320	2.00	42.6	0.29	26	325	2	1.900	70	1.720	1.470	0.770	1.64	5.95
153		160	320	2.00	42.6	0.29	26	325	2	1.900	71.7	1.810	1.500	0.790	1.68	6.26
154		160	320	2.00	42.6	0.29	26	325	3	1.900	75.5	2.100	1.400	0.730	1.77	7.27
155		160	320	2.00	42.6	0.29	26	325	3	1.900	78.8	2.490	1.500	0.780	1.85	8.62
156		160	320	2.00	42.6	0.29	26	325	3	1.900	77.5	2.240	1.430	0.750	1.82	7.75
157	160	320	2.00	61.7	0.31	26	325	1	1.900	77.5	1.110	1.600	0.840	1.26	3.57	
158	160	320	2.00	61.7	0.31	26	325	2	1.900	80.8	1.490	1.500	0.790	1.31	4.79	
159	160	320	2.00	61.7	0.31	26	325	2	1.900	76.7	1.350	1.420	0.740	1.24	4.34	
160	160	320	2.00	61.7	0.31	26	325	2	1.900	78	1.440	1.480	0.780	1.26	4.63	
161	160	320	2.00	61.7	0.31	26	325	3	1.900	90.1	1.710	1.350	0.710	1.46	5.50	
162	160	320	2.00	61.7	0.31	26	325	3	1.900	92.1	1.880	1.420	0.740	1.49	6.05	
163	160	320	2.00	61.7	0.31	26	325	3	1.900	94.4	1.950	1.500	0.790	1.53	6.27	

**E_r*: Elasticity modulus is given in KN/mm-ply; **f_r*: Tensile strength is given in N/mm-ply; **t_r*: Thickness is given in ply

Appendix 2

Table 2 Selected design-oriented strength and strain models

No.	Source	Strength equation	Strain equation	Type of confinement
1	Saadatmanesh <i>et al.</i> (1994)	$\frac{f'_{cc}}{f'_{co}} = -1.254 - 2\left(\frac{f_l}{f'_{co}}\right) + 2.254\sqrt{1 + 7.94\frac{f_l}{f'_{co}}}$	$\frac{\varepsilon_{cc}}{\varepsilon_{co}} = 1 + 5\left(\frac{f'_{cc}}{f'_{co}} - 1\right)$	GFRP and CFRP-confined concrete
2	Karbhari and Gao (1997)	$\frac{f'_{cc}}{f'_{co}} = 1 + 2.1\left(\frac{f_l}{f'_{co}}\right)^{0.87}$	$\frac{\varepsilon_{cc}}{\varepsilon_{co}} = 1 + \frac{0.01}{\varepsilon_{co}}\left(\frac{f_l}{f'_{co}}\right)$	FRP-wrapped concrete
3	Toutanji (1999)	$\frac{f'_{cc}}{f'_{co}} = 1 + 3.5\left(\frac{f_l}{f'_{co}}\right)^{0.85}$	$\frac{\varepsilon_{cc}}{\varepsilon_{co}} = 1 + (310.57\varepsilon_f + 1.9)\left(\frac{f'_{cc}}{f'_{co}} - 1\right)$	FRP-wrapped concrete
4	Moran and Pantelides (2002)	$\frac{f'_{cc}}{f'_{co}} = 1 + 4.14\left(\frac{f_l}{f'_{co}}\right)$	$\frac{\varepsilon_{cc}}{\varepsilon_{co}} = 1 + \frac{(f_l/f'_{co})}{9.27 \times 10^{-3} \left(\frac{E_l}{f'_{co}}\right)^{\frac{1}{3}}}$	FRP-confined concrete
5	Xiao and Wu (2003)	$\frac{f'_{cc}}{f'_{co}} = 1 + \left(4.1 - 0.45\left(\frac{E_l}{f'_{co}{}^2}\right)^{-1.4}\right)\left(\frac{f_{l,rup}}{f'_{co}}\right)$ $k_\varepsilon = 0.5 - 0.8$	$\frac{\varepsilon_{cc}}{\varepsilon_{co}} = \frac{\varepsilon_{h,rup} - 0.00047}{10\varepsilon_{co}} \times \left(\frac{E_l}{f'_{co}}\right)^{0.9}$ $k_\varepsilon = 0.5 - 0.8$	CFRP and GFRP-confined concrete
6	Bisby <i>et al.</i> (2005)	$\frac{f'_{cc}}{f'_{co}} = 1 + 3.587\left(\frac{f_l}{f'_{co}}\right)^{0.84}$	$\frac{\varepsilon_{cc}}{\varepsilon_{co}} = 1 + \frac{0.0137}{\varepsilon_{co}}\left(\frac{f_l}{f'_{co}}\right)$	CFRP, GFRP and AFRP-confined concrete
7	Mathys <i>et al.</i> (2005)	$\frac{f'_{cc}}{f'_{co}} = 1 + 3.5\left(\frac{f_{l,rup}}{f'_{co}}\right)^{0.85}$ $k_\varepsilon = 0.6$	$\frac{\varepsilon_{cc}}{\varepsilon_{co}} = 1 + (310.57\varepsilon_f + 1.9)\left(\frac{f'_{cc}}{f'_{co}} - 1\right)$ $k_\varepsilon = 0.6$	FRP-wrapped concrete
8	Berthet <i>et al.</i> (2006)	$\left\{ \begin{array}{l} \frac{f'_{cc}}{f'_{co}} = 1 + 3.45\left(\frac{f_{l,rup}}{f'_{co}}\right) \\ \text{for } 20 \text{ MPa} \leq f'_{co} \leq 50 \text{ MPa} \\ \frac{f'_{cc}}{f'_{co}} = 1 + 9.5\left(\frac{f_{l,rup}}{f'_{co}{}^{1.25}}\right) \\ \text{for } 50 \text{ MPa} \leq f'_{co} \leq 200 \text{ MPa} \end{array} \right.$	$\frac{\varepsilon_{cc}}{\varepsilon_{co}} = 1 + \frac{\varepsilon_{h,rup} - \nu_c \varepsilon_{co}}{\frac{1}{\sqrt{2}} \varepsilon_{co}} \times \left(\frac{E_l}{f'_{co}{}^2}\right)^{\frac{2}{3}}$ (ν_c) Poisson's ratio of concrete	CFRP and GFRP-wrapped concrete
9	Wu <i>et al.</i> (2006)	$\frac{f'_{cc}}{f'_{co}} = 0.408 + 6.157\frac{f_l}{f'_{co}} - 3.25\left(\frac{f_l}{f'_{co}}\right)^2$	$\frac{\varepsilon_{cc}}{\varepsilon_{co}} = \frac{\varepsilon_f}{0.56\varepsilon_{co}}\left(\frac{f_l}{f'_{co}}\right)^{0.66}$	FRP-wrapped concrete
10	Ciupala <i>et al.</i> (2007)	$\frac{f'_{cc}}{f'_{co}} = 1 + 3.4\left(\frac{f_l}{f'_{co}}\right)^{0.8}$	$\frac{\varepsilon_{cc}}{\varepsilon_{co}} = 1 + 6.7\left(\frac{f'_{cc}}{f'_{co}} - 1\right)^{\frac{2}{3}}$	CFRP and GFRP-confined concrete
11	Youssef <i>et al.</i> (2007)	$\frac{f'_{cc}}{f'_{co}} = 1 + 2.25\left(\frac{f_l}{f'_{co}}\right)^{1.25}$	$\frac{\varepsilon_{cc}}{\varepsilon_{co}} = \frac{0.003368}{\varepsilon_{co}} + \frac{0.2590}{\varepsilon_{co}}\left(\frac{f_f}{E_f}\right)^{\frac{1}{2}}\left(\frac{f_l}{f'_{co}}\right)$	CFRP and GFRP-confined concrete (circular and rectangular sections)
12	Fahmy and Wu (2010)	$\left\{ \begin{array}{l} \frac{f'_{cc}}{f'_{co}} = 1 + 4.5\left(\frac{f_l}{f'_{co}}\right)^{0.7} \\ \text{for } f'_{co} \leq 40 \text{ MPa} \\ \frac{f'_{cc}}{f'_{co}} = 1 + 3.75\left(\frac{f_l}{f'_{co}}\right)^{0.7} \\ \text{for } f'_{co} > 40 \text{ MPa} \end{array} \right.$	$\frac{\varepsilon_{cc}}{\varepsilon_{co}} = \frac{f'_{cc} - f'_{co}}{E_{c2}\varepsilon_{co}} \left(\frac{m_1}{m_2} + 0.6728E_f \right)$ $\left\{ \begin{array}{l} m_1 = 0.5, m_2 = 0.83, f'_{co} \leq 40 \text{ MPa} \\ m_1 = 0.2, m_2 = 1.73, f'_{co} > 40 \text{ MPa} \end{array} \right.$	FRP-wrapped concrete
13	Pham and Hadi (2014)	$\frac{f'_{cc}}{f'_{co}} = 0.91 + 1.88\frac{f_{l,rup}}{f'_{co}} + 7.6\frac{t_f}{d f'_{co}}$	$\frac{\varepsilon_{cc}}{\varepsilon_{co}} = 1 + \frac{13.24(t_f f_f \frac{\varepsilon_{h,rup}}{\varepsilon_{co}})}{(d f'_{co} + 3.3 f_f t_f)}$	FRP-wrapped concrete
14	Sadeghian and Fam (2015)	$\frac{f'_{cc}}{f'_{co}} = 1 + (2.77\rho_K^{0.77} - 0.07)\rho_\varepsilon^{0.91}$	$\frac{\varepsilon_{cc}}{\varepsilon_{co}} = 1.5 + 6.78\rho_K^{0.63}\rho_\varepsilon^{1.08}$	FRP-confined concrete
15	Touhari and Mitiche-Kettab (2016)	$\frac{f'_{cc}}{f'_{co}} = 1 + 1.85\left(\frac{f_l}{f'_{co}}\right)$ $k_\varepsilon = 0.74$	$\frac{\varepsilon_{cc}}{\varepsilon_{co}} = 1.45 + 15\left(\frac{f_l}{f'_{co}}\right)$ $k_\varepsilon = 0.74$	GFRP-wrapped concrete
16	Huang <i>et al.</i> (2016)	$\frac{f'_{cc}}{f'_{co}} = 1 + 1.69\left(\frac{f_{l,rup}}{f'_{co}}\right)^{0.63}$	$\frac{\varepsilon_{cc}}{\varepsilon_{co}} = 1 + 13.2\left(\frac{f_{l,rup}}{f'_{co}}\right)^{0.6}$	GFRP-wrapped concrete and concrete-filled GFRP tube
17	Baji <i>et al.</i> (2016)	$\frac{f'_{cc}}{f'_{co}} = 1 + 3.29\left(\frac{f_{l,rup}}{f'_{co}}\right)$ $k_\varepsilon = 0.66$	$\frac{\varepsilon_{cc}}{\varepsilon_{co}} = 1 + 0.54\left[\left(\frac{1}{5.1}\right)\left(\frac{\varepsilon_{h,rup}}{\varepsilon_{co}}\right)\left(\frac{E_l}{f'_{co}}\right)^{0.56}\right]$ $k_\varepsilon = 0.66$	FRP-wrapped concrete

Table 2 Continued

No.	Source	Strength equation	Strain equation	Type of confinement
18	Lim <i>et al.</i> (2016)	$\frac{f'_{cc}}{f'_{co}} = \frac{1 + E_l \varepsilon_{h,rup} + E_l^{1.5} \varepsilon_{h,rup}^2 + a}{f'_{co}}$ $a = \sqrt{E_l - \frac{f'_{co}}{\sqrt{\varepsilon_{h,rup}}}} \geq 0$	$\frac{\varepsilon_{cc}}{\varepsilon_{co}} = \left(1 + \frac{b}{\varepsilon_{co}}\right) \left(\varepsilon_{co}^c + \frac{E_l}{f'_{co}} (2\varepsilon_{co} + b)\right)$ $b = \varepsilon_{h,rup} - \varepsilon_{h,rup} \frac{E_l}{f'_{co}};$ $c = f'_{co} (\varepsilon_{co} + \varepsilon_{h,rup} + e^{\varepsilon_{h,rup}}) / E_l$ $\varepsilon_{h,rup} = \varepsilon_f / f'_{co}{}^{0.125};$ $\varepsilon_{co} = (f'_{co}{}^{0.225} / 1000) k_s k_a$ $k_s = (152/d)^{0.1}; k_a = (2d/h)^{0.13}$	FRP-wrapped concrete
19	Keshtegar <i>et al.</i> (2017)	$\frac{f'_{cc}}{f'_{co}} = 1 + (0.85 + 1.40\rho_\varepsilon)\rho_a^{0.82}\rho_E^{0.91}$ $\rho_a = \frac{t_f}{d}, \rho_E = \frac{2E_f}{f'_{co}/\varepsilon_{co}}$	$\frac{\varepsilon_{cc}}{\varepsilon_{co}} = 1.5 + (-0.09 + 3.27\rho_a^{0.4})\rho_E^{0.6}\rho_\varepsilon^{1.04}$ $\rho_a = \frac{t_f}{d}, \rho_E = \frac{2E_f}{f'_{co}/\varepsilon_{co}}$	FRP-wrapped concrete
20	Fallah Pour <i>et al.</i> (2018)	$\frac{f'_{cc}}{f'_{co}} = 1 + \frac{(2.5 - 0.01f'_{co})E_l\varepsilon_f}{f'_{co}}$	$\frac{\varepsilon_{cc}}{\varepsilon_{co}} = 1.5 + (0.3 - 0.001f'_{co}) \left(\frac{E_l}{f'_{co}}\right)^{0.75} \frac{\varepsilon_f^{1.35}}{\varepsilon_{co}}$	FRP-confined concrete